

## MODELING OF RESIDUAL STRESSES IN HY-100 WELDMENTS

CONF-970558--2

T. Zacharia, B. Taljat, and B. Radhakrishnan  
Modeling and Simulation Group, Metals and Ceramics Division  
Oak Ridge National Laboratory, Oak Ridge, TN 37831-6140

RECEIVED

JAN 28 1997

OSTI

### ABSTRACT

The residual stress distribution in a HY-100 steel disk, induced by gas tungsten arc (GTA) spot welding, was analyzed using finite element (FE) formulations and measured with the neutron diffraction technique. The computations used temperature-dependent thermophysical and mechanical properties. The predictions from the FE models are in very good agreement with the neutron diffraction measurements in the far heat affected zone (HAZ) and in the base metal. The predicted residual stresses in the fusion zone and the near HAZ were higher than those measured by the neutron diffraction method. This discrepancy was attributed to the microstructural changes and associated material properties in the HAZ and fusion zone due to phase transformations during the weld thermal cycle.

### INTRODUCTION

MASTER

Some major problems in welded structures are residual stresses and distortion. Residual stresses that develop in and around the welded joint are detrimental to the integrity and the service behavior of the welded part. High tensile residual stresses in the region near the weld might promote brittle fracture, change or aid the fatigue strength and stress corrosion cracking. Not only can they combine with stresses from service but even before the weldment sees service, residual stresses can lead to crack formation and failure of the structural member.

Residual stresses develop in a material due to uneven distribution of inelastic strains caused by localized heating during welding and subsequent uneven cooling of the material. Due to localized heating, complex thermal and transformation stresses are generated during welding. Several factors may contribute to the formation of residual stresses (Smith, et al., 1989; Murti, et al., 1993; Balaguer, et al., 1989; Mahin, et al., 1991; Roelens, 1996). The plastic deformation produced in the base metal is a function of structural, material, and fabrication parameters. Structural parameters include geometry, thickness, and joint design. Material parameters reflect the metallurgical condition of the base material and the weld filler metal. Fabrication parameters include welding process, procedure, parameters, and the degree of restraint.

The objective of this study is to analyze the residual stress state in an HY-100 disk after the welding process. A finite element (FE) model was developed for residual stress analysis in spot welds. Results of the analysis were compared with carefully conducted neutron diffraction measurements (Feng, et al., 1995).

DISTRIBUTION OF THIS DOCUMENT IS UNRESTRICTED

The submitted manuscript has been authored by a contractor of the U.S. Government under contract No. DE-AC05-96OR22464. Accordingly, the U.S. Government retains a nonexclusive, royalty-free license to publish or reproduce the published form of this contribution, or allow others to do so, for U.S. Government purposes.

ph

## DISCLAIMER

This report was prepared as an account of work sponsored by an agency of the United States Government. Neither the United States Government nor any agency thereof, nor any of their employees, make any warranty, express or implied, or assumes any legal liability or responsibility for the accuracy, completeness, or usefulness of any information, apparatus, product, or process disclosed, or represents that its use would not infringe privately owned rights. Reference herein to any specific commercial product, process, or service by trade name, trademark, manufacturer, or otherwise does not necessarily constitute or imply its endorsement, recommendation, or favoring by the United States Government or any agency thereof. The views and opinions of authors expressed herein do not necessarily state or reflect those of the United States Government or any agency thereof.

## **DISCLAIMER**

**Portions of this document may be illegible  
in electronic image products. Images are  
produced from the best available original  
document.**

## EXPERIMENTAL

A GTA welding process without filler metal was used to make a spot weld on a HY-100 steel disk. The disk measured 19mm in height and 75mm in diameter. The weld was located at the center of the disk surface. The following welding parameters were used: Electric current  $I = 320\text{A}$ , voltage  $U = 15\text{V}$ , and 4mm electrode diameter. Welding arc time was 5s with argon shielding and followed by a 5 seconds post purge. No constraint was used during welding and subsequent cooling. Figure 1 shows the welding setup.

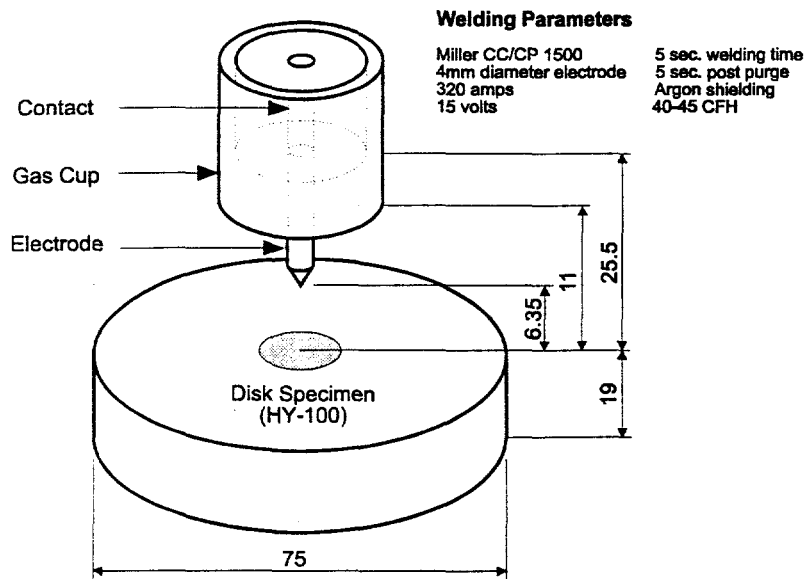


Figure 1. Welding setup.

Neutron diffraction measurements were performed on the BEAM Tube-6 (BT-6) triple-axis spectrometer at the National Institute of Standard and Technology Research Reactor. Measurements were made using a nominal gauge volume of  $3 \times 3 \times 3 \text{ mm}$ . Figure 2 shows the positions and relative sizes of the measurement points which are located on the radial section plane. Instrument details and measurement methodology have been discussed elsewhere (Prask, et. al., 1991; Brand, et. al., 1994).

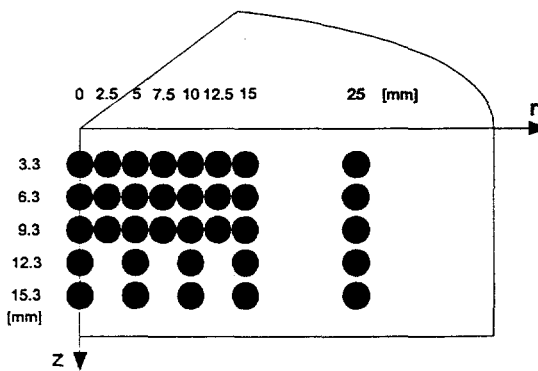


Figure 2. HY-100 disk with ND measurement locations.

## RESULTS AND DISCUSSION

The residual stress distribution in a GTA spot welded HY-100 steel disk was analyzed using thermo-mechanically uncoupled FE formulation. The computations used temperature-dependent thermo-physical and mechanical properties of the base metal (BM). The thermal analysis was based on the heat conduction formulation with the Gaussian heat input from the arc. An axisymmetric FE model was developed which considerably simplifies the modeling effort. One half of the actual disk cross section was meshed by linear four-noded finite elements. Computations were performed by using a general purpose FE code.

Two computational steps are required to compute the residual stresses in welding. In the first step, the heating/melting of the material is modeled by applying the heat flux. Cooling transients are calculated in the second step when the heat source is removed and the disk is cooled to room temperature. The heating time is five seconds, whereas the disk is cooled until the isotherm ambient temperature is reached. Figure 3 shows temperature profiles at specific distances from the weld centerline.

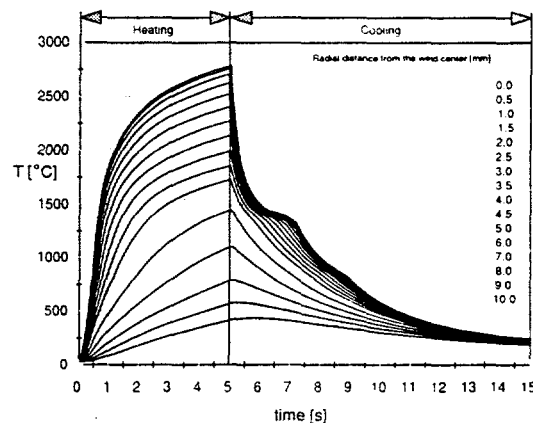


Figure 3. Temperature transient at depth of 1 mm.

Rate-independent, elasto-plastic constitutive equations were constructed from the uniaxial tensile test results of the base metal under various temperature conditions. Both yield and ultimate stresses were reduced to 5.0 MPa at the melting temperature to simulate low strength at high temperatures. Elastic modulus and Poisson's ratio were also given as a function of temperature. The elastic modulus was reduced to a small value (1.0 GPa) at high temperatures. Phase transformation effects due to rapid cooling on mechanical properties of carbon steel were not included at this stage of the analysis.

The same FE mesh as in the thermal analysis was used in the mechanical analysis, except for the element type and different boundary conditions. The analysis is based on the temperature gradients calculated in the thermal analysis which represent the input information or loading. The disk was restrained in the axial direction on the bottom surface to appropriately model the actual welding conditions.

Residual stresses and elastic strains were evaluated after the welding process was completed and disk had cooled to room temperature. Comparison with the ND results was made at this point and is shown in Fig. 4.

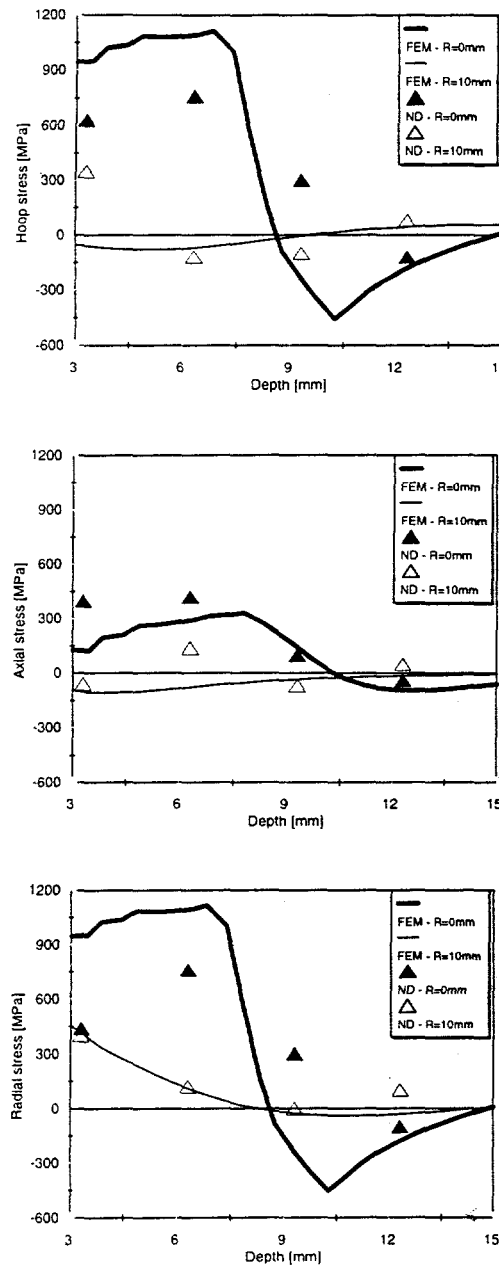


Figure 4. Comparison of FE and ND results in radial, axial, and tangential direction.

tion ( $\epsilon_{tr}$ ) to the constitutive thermal expansion curve of HY-100 ( $\epsilon_\gamma$ ). Figure 5 shows the overall thermal expansion coefficient of HY-100 ( $\alpha_{tot}$ ), which corresponds to  $\epsilon_{tot}$ . Note that in this case the reference temperature for defining the thermal expansion coefficient equals the melting temperature.

The predictions of the finite element model are in good agreement with the neutron diffraction residual stress results in the far heat affected zone (HAZ) and BM. The model overpredicted the actual residual stress field in the fusion zone and the near HAZ.

The discrepancy was attributed to the phase transformations and associated changes in material properties in the HAZ and fusion zone (FZ), that occur during welding thermal cycle. Martensitic transformations that occur in the FZ and HAZ have opposite effects on the residual stress. The higher yield strength tends to increase the residual stress level in the FZ and HAZ since these areas experience plastic deformation. At the same time, the associated volume expansion tends to minimize the effect of thermal contraction thereby reducing the residual stress level in the FZ and HAZ. The formation of cracks in the FZ is another factor that possibly contributes to lower measured residual stress values.

Based on these initial results, a model was developed to study the effect of volumetric changes that occur during phase transformation on residual stress. At this stage, the volume change was approximated by the introduction of a modified thermal expansion coefficient. The thermal expansion coefficient for the austenitic phase ( $\alpha_\gamma$ ) was modified with a coefficient  $\alpha_{tr}$ , which simulated a linear increase in volume at a certain temperature range due to the presence of the martensitic phase. The overall thermal expansion ( $\epsilon_{tot}$ ) was obtained by superimposing the thermal expansion due to phase transforma-

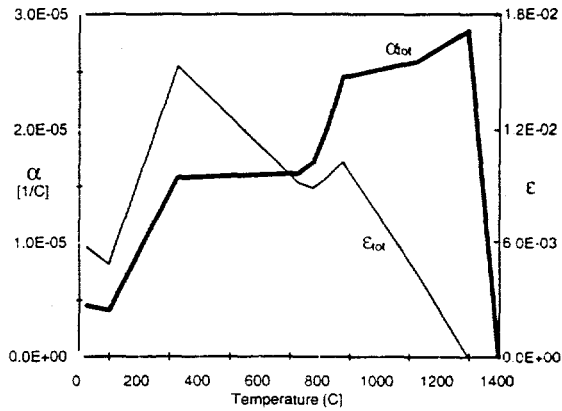


Figure 5. Thermal expansion coefficient,  $\alpha_{\text{tot}}$ .

The effect of phase transformation on the weld volume change was analyzed with respect to the quantity of transformed product. An average weld volume increase of 1% at the transformation temperature range was assumed. The actual expansion in HAZ and FZ depends upon the volume fraction of martensite, which is a function of the local cooling rates, local grain size, and local composition of the austenite. Comparison of the calculated and ND results are presented in Figs. 6-8 for the weld centerline ( $R = 0$ ) indicating good agreement.

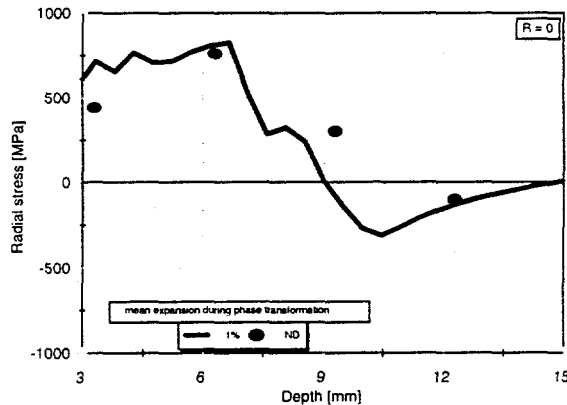


Figure 6. FE and ND radial stress at  $R = 0$ .

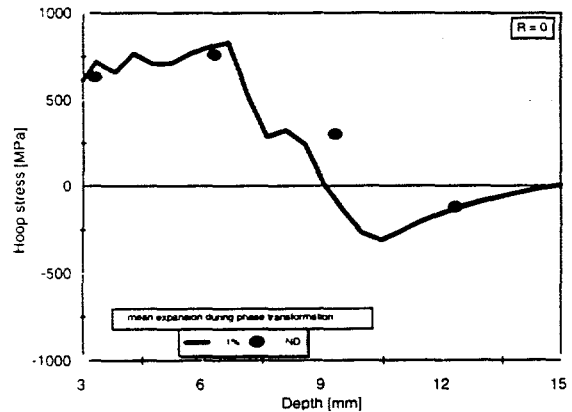


Figure 7. FE and ND hoop stress at  $R = 0$ .

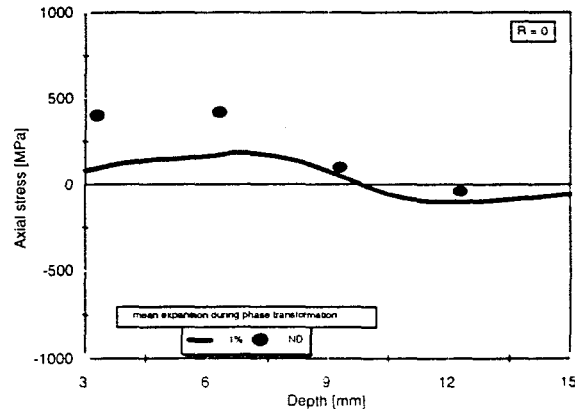


Figure 8. FE and ND axial stress at  $R = 0$ .

## CONCLUSIONS

The predicted residual stresses are in very good agreement with the neutron diffraction measurements. The results show a significant effect of volume change due to phase transformation on residual stresses in the FZ and the HAZ. The model tends to over-predict the measured residual stresses in the FZ and the near HAZ when the effect of phase transformation and associated change in the material properties are not included. The overall agreement of FE residual stress results, assuming 1% volume increase in the weld region, and ND results is very good.

## ACKNOWLEDGMENTS

The authors thank Drs. S. Simunovic and X.-L. Wang of Oak Ridge National Laboratory for reviewing the paper. Research sponsored by the Division of Materials Sciences, U.S. Department of Energy, under contract DE-AC05-96OR22464 with Lockheed Martin Research Corporation, and by the U.S.Navy, Office of Naval Research, under interagency agreement DOE No. 1866-E126-A1, Navy No. N000014-92-0063 under Department of Energy contract DE-AC05-96OR22464 with Lockheed Martin Research Corporation.

## REFERENCES

Balaguer, J. P.; Wang, Z.; and Nippes, E. F. (1989): Stress-Relief Cracking of a Copper-Containing HSLA Steel, Welding Research Supplement, April, pp.121-131

Brand, P. C., Prask, H. J., Blackburn, J., Fields, R. J., and Proctor, T. M., (1994), Proc. of the MRS Fall Meeting in Boston.

Feng, Z.; Zhu, Y. Y.; Zacharia, T.; Fields, R. J.; Brand, P. C.; Prask, H. J.; and Blackburn, J. M. (1995): Modeling and Validation of Residual Stress Distribution in an HSLA-100 Disk, Proceedings of 4th International Conference on Trends in Welding Research, Gatlinburg TN

Mahin, K. W.; Winters, W.; Holden, T. M.; Hosbous, R. R.; and MacEwen, S. R. (1991): Prediction and Measurement of Residual Elastic Strain Distributions in Gas Tungsten Arc Welds, Welding Research Supplement, September, pp. 245 - 254

Murti, V. S. R.; Srinivas, P. D.; Banadeki, G. D. H.; and Raju, K. S. (1993): Effect of Heat Input on the Metallurgical Properties of HSLA Steel in Multi-Pass MIG Welding, Journal of Materials Processing Technology, Vol. 37, pp. 723-729

Prask, H. J. and Choi, C. S. (1991) Practical Applications of Residual Stress Technology, (ed, C. Ruud), ASM International, Metals Park, OH 1991, 87-93.

Roelens, J. B. (1996): Numerical Simulation of Some Multipass Submerged Arc Welding Determination of the Residual Stresses and Comparison With Experimental Measurements, The Eight International Conference on Pressure Vessel Technology, Montreal, Canada

Smith, N. J.; McGrath, J. T.; Gianetto, J. A.; and Orr, R. F. (1989): Microstructure/Mechanical Property Relationships of Submerged Arc Welds in HSLA 80 Steel, Welding Research Supplement, March, pp.112-120